The Neuregulin1/ErbB system is selectively regulated during peripheral nerve degeneration and regeneration

The Neuregulin1/ErbB system is selectively regulated during peripheral nerve degeneration and regeneration

Giulia Ronchi[1,2], Kirsten Haastert-Talini[3], Benedetta Elena Fornasari[1], Isabelle Perroteau[1,4], Stefano Geuna[1,2,4] and Giovanna Gambarotta[1,4]

[1] Department of Clinical and Biological Sciences, University of Torino, Italy;
[2] Neuroscience Institute of the "Cavalieri Ottolenghi" Foundation (NICO), University of Torino, Italy;
[3]Institute of Neuroanatomy, Hannover Medical School, and Center for Systems Neuroscience (ZSN), Hannover, Germany;
[4] Neuroscience Institute of Torino (NIT), University of Torino, Italy.

Running title: nerve injury, remyelination, gene expression, NRG1/ErbB

Number of pages: 32
Number of figures: 9
Number of tables: 1
Number of words in the whole manuscript: 10518
Number of words in the Abstract: 249
Number of words in the Introduction: 480

Keywords: nerve injury, remyelination, NRG1/ErbB, biomolecular analysis, electron microscopy

Corresponding author: Giovanna Gambarotta
Dipartimento di Scienze Cliniche e Biologiche
Università di Torino
Ospedale San Luigi
Regione Gonzole 10
10043 - Orbassano (TO), ITALY
Telephone: +39.011.6705433
FAX: +39.011.9038639
e-mail:giovanna.gambarotta@unito.it

Abstract

The peripheral nervous system has an intrinsic capability to regenerate that is crucially related to the ability of Schwann cells (SC) to create a permissive environment, e.g. through production of regeneration promoting neurotrophic factors. Survival, proliferation, migration and differentiation of SC into a myelinating phenotype during development and after injury is regulated by different Neuregulin1 (NRG1) isoforms.

This study investigates the expression of different NRG1 isoforms and of their ErbB receptors in distal rat median nerve samples under regenerating conditions after a mild (crush) and more severe (end-to-end repair) injury and under degenerating condition. The expression of the NRG1/ErbB system was evaluated at mRNA and protein level and demonstrated to be specific for distinct and consecutive phases following nerve injury and regeneration or the progress in degeneration. For the first time we present a detailed analysis of expression profiles not only of soluble and transmembrane NRG1 isoforms, but also of alpha and beta as well as type a, b, and c isoforms. The results of mRNA and protein expression pattern analyses were related to nerve ultrastructure changes evaluated by electron microscopy.

In particular, transmembrane NRG1 isoforms are differentially regulated under regeneration and degeneration conditions. Soluble NRG1 isoforms alpha and beta, as well as type a and b, are strongly up-regulated during axonal regrowth, while type c NRG1 isoform is down-regulated. This is accompanied by an up-regulation of ErbB receptors.

This accurate regulation suggests that each molecule plays a specific role that could be clinically exploited to improve nerve regeneration.

Introduction

Following an injury to the Peripheral Nervous System (PNS), nerve fibres retain the capacity to regenerate. However, a complete repair is rarely achieved, leading to a partial or total loss of motor, sensory and autonomic functions.

Peripheral nerve degeneration and regeneration involve complex processes such as morphological and physiological modifications, variation in cellular composition and changes in gene expression and signal transduction. Investigating these mechanisms on a molecular level is therefore important to identify factors promoting successful nerve repair, especially axonal regrowth, remyelination, and target reinnervation.

It is well known that peripheral glia cells, Schwann cells (SC), are the crucial element to create an environment supportive for axonal regeneration. Thus recognizing signals that control the SC response in nerve regeneration and degeneration is of great interest. One of the most important factors regulating SC action is Neuregulin1 (NRG1), which is not only involved in survival, proliferation, differentiation, and migration of SC during development, but is also required for axon guidance by SC and remyelination after nerve injury in adulthood (Taveggia *et al.*, 2010; Fricker & Bennett, 2011; Pereira *et al.*, 2012; Salzer, 2012; Gambarotta *et al.*, 2013; Heermann & Schwab, 2013; Gambarotta *et al.*, 2014b).

The gene coding for NRG1 is very large and through the use of different promoters and alternative exon splicing, a vast variety of distinct transcripts and protein isoforms are generated (Adlkofer & Lai, 2000). According to their structure and signalling activity, NRG1 isoforms can be classified as soluble or transmembrane. Soluble isoforms (type I/II) are produced as pro-NRG1 anchored to the cell membrane. Following a proteolytic cleavage, a soluble fragment is released into the extracellular environment for paracrine or autocrine signalling. Transmembrane isoforms (type III) signal in a juxtacrine manner. The NRG1 isoforms can be further divided into alpha and beta isoforms, according to the presence of a small domain downstream the EGF like domain, and into type a, b, and c isoforms, according to the exon present in the C-terminal tail (Falls, 2003).

NRG1 signalling is transduced in SC by ErbB2/ErbB3 heterodimers (Garratt *et al.*, 2000; Yarden & Sliwkowski, 2001). NRG1 isoforms have different spatiotemporal patterns of expression providing different roles during myelination and nerve repair. When expressed by axons, transmembrane NRG1 determines their myelination status and the

myelin sheath thickness, both during development and nerve regeneration (Michailov et al., 2004; Taveggia et al., 2005). In contrast, autocrine signalling via soluble NRG1 is not necessary for developmental myelination, but for SC survival, redifferentiation and remyelination after nerve injury (Stassart et al., 2013).

In this study we elucidate changes in mRNA and protein expression of NRG1, ErbB receptors, and myelin basic protein during early peripheral nerve regeneration and degeneration. Therefore, adult rat median nerves were crushed or end-to-end repaired (regenerating conditions) or left unrepaired after transection (degenerating condition) and distal nerve segments were subjected to expression analysis. Additionally, nerve morphology analysis revealed the morphological correlates.

Material and Methods

Ethical standards

All procedures were approved by the Bioethics Committee of the University of Torino, by the Institutional Animal Care and Use Committee of the University of Torino, and by the Italian Ministry of Health, in accordance with the European Communities Council Directive of 24 November 1986 (86/609/EEC).

Surgery

In this study a total of 64 adult female Wistar rats (Harlan Laboratories), weighing approximately 200 g, were used. Animals were housed in plastic cages with free access to food and water; their room was maintained at constant temperature and humidity under 12–12 h light/dark cycles.

For mRNA and protein analysis, a total of 52 rats were randomly divided into 4 experimental groups according to the nerve injury/repair: (i) in the crush injury group (axonotmesis), median nerves were bilaterally crushed at the mid humerus level with a non-serrated clamp, as previously described (Ronchi et al., 2009); (ii) for end-to-end repair (neurotmesis) median nerves were bilaterally transected at the same position as in (i) and the proximal and distal nerve ends were immediately reconnected with two epineurial sutures (9/0); (iii) in the degenerating nerve group, median nerves were bilaterally transected at the same location as in (i) and (ii) and left unrepaired (to prevent regeneration, the proximal stumps were sutured to the major pectoralis muscle); (iv) finally, in the control group (n=7), animals were left uninjured.

For electron microscopy analysis (nerve morphology), 5 additional rats were subjected to condition (i) and 5 rats to condition (iii). Finally, for in vitro nerve culture, 2 rats were used.

During surgery, rats were deeply anesthetized with Tiletamine and Zolazepam (Zoletil) i.m. (3 mg/kg). Adequate measures were taken to minimize pain and discomfort during the post-operative period.

Rats were sacrificed by lethal i.m. injection of Tiletamine and Zolazepam at different time-points after injury/repair/degeneration. For mRNA and protein analysis, n=3 animals per time-point were analysed. For morphological analysis, n=1 animal per time-point was sacrificed. Time points analysed were: 1, 3, 7, 14 and 28 days. Nerve segments

(approximately 10mm) distally to the lesion site were collected. Control nerves were collected from healthy animals.

In vitro *nerve culture*

For *in vitro* nerve degeneration, each median nerve was divided into two 5-mm segments and cultured for 1 day in high glucose DMEM (Sigma) supplemented with 100 units/ml penicillin, 0.1 mg/ml streptomycin, 1 mM sodium pyruvate, 2 mM L-glutamine, 10% heat-inactivated foetal bovine serum (FBS, Invitrogen). Nerves were grown at 37°C in a 5% CO_2 atmosphere saturated with H_2O.

RNA isolation, cDNA preparation and quantitative real-time PCR

Total RNA was isolated using the TRIzol Reagent (Invitrogen) according to the manufacturer's instructions. 0.75 µg total RNA were subjected to a reverse transcriptase (RT) reaction in a 20 µl reaction volume containing: 1x RT-Buffer (Invitrogen), 0.1 µg/µl bovine serum albumin (BSA), 0.5 µM dNTPs; 7.5 µM random decamers (Invitrogen); 40 U RIBOlock (Fermentas) and 200 U SuperScript III Reverse Transcriptase (Invitrogen). The reaction was performed at 25°C 10 min, at 50°C 90 min, at 70°C 15 min. Quantitative real-time PCR was performed using an ABI Prism 7300 (Applied Biosystems, Life Technologies Europe BV, Monza, Italy) detection system. cDNA was diluted 12.5 fold in nuclease-free water and 5 µl (corresponding to 15ng starting RNA) were analysed in a 20 µl reaction volume, containing 1 x iTaq Universal SYBR Green Supermix (BioRad) and 300 nM forward and reverse primers. Dissociation curves were routinely performed to check for the presence of a single peak corresponding to the required amplicon. Analysis was performed in technical and biological triplicate.

The data from the real-time PCR experiments were analysed using the ΔΔCt method for the relative quantification. The threshold cycle number (Ct) values of both the calibrator and the samples of interest were normalized to the geometric average of two endogenous housekeeping genes: ANKRD27 (Ankyrin repeat domain 27) and RICTOR (RPTOR Independent Companion Of MTOR, Complex 2) (Gambarotta *et al.*, 2014a). As calibrator the average of uninjured nerves was used.

Primers were designed using Annhyb software (http://www.bioinformatics.org/annhyb/) and synthesized by Invitrogen (Life Technologies Europe BV, Monza, Italy). Primers sequences are reported in Table I.

All normalized relative quantitative data are depicted in the results section as -ΔΔCT instead of $2^{-\Delta\Delta CT}$ because in this way it is possible to appreciate both up-regulation (ranging between 0 and + ∞) and down-regulation (ranging between 0 and - ∞), while, when data are expressed as the more commonly used $2^{-\Delta\Delta CT}$, the down-regulation is graphically compressed (ranging between 0 and +1).

Total protein extraction and western blot analysis

Total proteins were extracted using the TRIzol Reagent (Invitrogen) after RNA extraction, according to the manufacturer's instructions. In the final passage, the protein pellet was re-suspended in boiling Laemli buffer (2.5% SDS, 0.125M TrisHCl pH6.8). Protein concentration was determined using the Bicinchoninic Acid assay kit (Sigma) on 1:4 diluted proteins to avoid detergent interference. Proteins (50µg/sample) were routinely resolved by 8% SDS-PAGE; for the analysis of NRG1 isoforms 4-15 % precast gels were used (Bio-Rad). Western blot analysis was carried out as previously described (Gambarotta *et al.*, 2004). Primary antibodies used were: anti-ErbB1 (#sc-03), anti-ErbB2 (#sc-284), anti-ErbB3 (#sc-285), anti-NRG1 type "a" C-terminal (#sc-348), (1:1000, all Santa Cruz, USA); anti-NRG1 type III N-terminal (#AB5551, 1:1000, Chemicon International, USA); anti-p-AKT (#4051), anti-AKT (#9272), anti-p-ERK (#9106), anti-ERK (#9102) (1:1000, all Cell Signaling Antibodies, MerckMillipore Europe); a pool of anti-MBP was used (#SMI 94 and SMI 99, 1:4000, Covance, Princeton, NJ, USA); anti-GAPDH (#4300, 1:20000, Ambion, ThermoFischer Scientific Inc, Europe); anti-β-actin (#A5316, 1:4000, Sigma, Germany); secondary antibodies used were horseradish peroxidise linked anti-rabbit (#NA934) and anti-mouse (#NA931) (both 1:40000, GE Healthcare Life Sciences, Europe).

Two housekeeping genes, actin and GAPDH, were shown in the western blot panels because, as discussed in a previous paper focused on housekeeping gene stability at mRNA level (Gambarotta *et al.*, 2014a), it is difficult to find a gene whose expression is not influenced by the injury.

Proteins previously extracted from primary cultured SC (Gnavi *et al.*, 2015) were used as a control for NRG1 expression.

Resin embedding and electron microscopy analysis

Nerve samples were fixed by immediate immersion in 2.5% glutaraldehyde in 0.1 M phosphate buffer (pH 7.4) for 4 to 6 hours at 4° C. Samples were then post-fixed in 2% osmium tetroxide for 2 hours and dehydrated in passages in ethanol from 30% to 100%. After two passages of 7 min each in propylene oxide and o/n in a 1:1 mixture of propylene oxide and Glauerts' mixture of resins, specimens were embedded in Glauerts' mixture of resins (made of equal parts of Araldite M and the Araldite Harter, HY 964). In the resin mixture, 0.5% of the plasticizer dibutylphthalate was added. For the final step, 2% of accelerator 964 was added to the resin in order to promote the polymerization of the embedding mixture.

Ultra-thin sections (70nm thick) were cut with an Ultracut UCT ultramicrotome (Leica Microsystems, Wetzlar, Germany) starting from the distal end and stained with saturated aqueous solution of uranyl acetate and lead citrate. Sections were analysed using a JEM-1010 transmission electron microscope (JEOL, Tokyo, Japan) equipped with a Mega-View-III digital camera and a Soft-Imaging-System (SIS, Münster, Germany) for the computerized acquisition of the images.

Statistical methods

Gene expression analysis was carried out in technical triplicates of biological triplicates. Data statistical analysis (one-way ANOVA with Bonferroni's post hoc) was performed using SPSS software. Data discussed in the paper refer to the comparison between the gene expression at different time points and the gene expression in the healthy nerve. Statistical analysis shown in the figures refers to the comparison among the three experimental models at the different analysed time points, as indicated in the figure legends.

Results

At the different time points after injury (1, 3, 7, 14, and 28 days) mRNA and protein expression levels of ErbB receptors and different NRG1 isoforms were examined by quantitative real-time PCR (qRT-PCR) and western blot analysis in median nerve segments obtained from healthy animals or distal nerve segments obtained from the three experimental groups: i) crush injury, ii) end-to-end repair, iii) degenerating nerve.

ErbB mRNAs are differentially regulated between regenerating and degenerating conditions

ErbB1 mRNA expression does not change significantly in the crush and degenerating groups following injury, whereas in the end-to-end group an up-regulation (1.73 ± 0.11 fold) is detectable at day-14 ($p=0.008$). At day-28 mRNA levels are comparable to control condition in the three experimental models (crush: 1.28 ± 0.21 fold; end-to-end: 1.45 ± 0.24 fold; degenerating nerve: 0.99 ± 0.16). Statistical analysis revealed significant effects related to the type of injury (Figure 1).

ErbB2 mRNA expression level demonstrates a strong down-regulation from day-1 after injury under regenerating conditions (crush: 0.29 ± 0.06 fold, $p<0.001$; end-to-end: 0.19 ± 0.03 fold, $p<0.001$) that lasts until day-28 (crush: 0.17 ± 0.04 fold, $p=0.034$; end-to-end: 0.51 ± 0.10 fold, $p<0.001$). Under degenerating conditions ErbB2 expression does not change significantly. Significant differences among groups are detectable (Figure 1).

ErbB3 mRNA expression is strongly decreased 1 day after injury (crush: 0.42 ± 0.12, $p=0.009$; end-to-end: 0.35 ± 0.09, $p=0.005$; degenerating nerve: 0.54 ± 0.14, $p=0.053$), followed by an increase until day-7 in all experimental groups.

Under regenerating conditions ErbB3 expression returns to control levels at day 28 (crush: 1.14 ± 0.19 fold; end-to-end repair: 1.61 ± 0.33 fold). Under degenerating conditions the up-regulation remains almost stable until day 28 after injury (2.84 ± 0.82, $p=0.001$). Statistical analysis showed significant differences related to the type of injury (Figure 1).

ErbB4 mRNA expression was also analysed, but in the peripheral nerve it is barely detectable (data not shown).

mRNA expression levels of NRG1 soluble isoforms are strongly up-regulated immediately after nerve injury

The mRNA expression of soluble isoforms of NRG1 (NRG1 type I/II, mostly expressed by SC), shows a similar time course pattern in all experimental models: expression is highly increased ($p<0.001$) immediately after injury, peaking at day-1 after injury (crush: 24.12 ± 6.02 fold; end-to-end: 26.75 ± 0.33 fold; degenerating nerve: 33.03 ± 6.03 fold). Then, the expression level decreases and returns to control values at day-28 after the injury. Intriguingly, in the degenerating group NRG1 type I/II expression is still higher at day-3 compared to control conditions (8.21 ± 2.10 fold, $p=0.002$) Statistical analysis revealed no significant effects among injury types (Figure 2).

Soluble and transmembrane NRG1 can be either the isoform alpha or beta, according to the exon present in the C-terminal region of the EGF-like domain. The expression of mRNA encoding for NRG1 alpha and NRG1 beta demonstrated a different regulation pattern.

Expression of NRG1 alpha is strongly up-regulated immediately after nerve injury in all experimental groups ($p<0.001$) displaying a peak at day-1 after injury (crush: 34.76 ± 12.45 fold; end-to-end: 36.80 ± 2.82 fold; degenerating nerve: 15.24 ± 3.73 fold). Under regenerating conditions, the expression level decreases towards control level which is reached and stabilized from day-14 to day-28 after injury. Under degenerating conditions a decrease of expression reaching control values at day-7 after injury is detectable, remaining not significantly different until day-28. Significant differences among the groups are not detectable (Figure 2).

Expression of NRG1 beta mRNA is also strongly up-regulated ($p<0.001$) peaking at day-1 after injury (crush: 12.18 ± 3.35 fold; end-to-end: 16.47 ± 0.37 fold; degenerating nerve: 13.55 ± 2.66 fold). In the following, the mRNA expression in the crush group reaches control expression levels already at day-3; in the end-to-end group mRNA expression decreases below control levels at day-7 (0.30 ± 0.12 fold, $p=0.046$) and day-14 (0.13 ± 0.00, $p=0.002$); finally, under degenerating conditions NRG1 beta expression is still up-regulated at day-3 (3.74 ± 1.06, $p=0.043$) and down-regulated at day-7 (0.17 ± 0.07,

p=0.001). Statistical analysis showed no significant differences related to the type of injury (Figure 2).

mRNA expression level of NRG1 transmembrane isoforms is regulated under regenerating conditions

Transmembrane NRG1 is known to be mainly expressed by axons, whose cell bodies are in the dorsal root ganglia and in the ventral horn of the spinal cord where mRNA transcription occurs. For this reason, in the healthy and injured nerves NRG1 type III transcript level is low, with high expression variability. Expression levels in the degenerating nerve do not change significantly, whereas they decrease under regenerating conditions at day-14 in the crush group (0.10 ± 0.01 fold, p=0.001) and at day-28 in the end-to-end group (0.07 ± 0.02 fold, p<0.001). Statistical analysis revealed significant effects related to the type of injury (Figure 2).

mRNA expression level of NRG1 type a, type b and type c isoforms is deeply regulated following nerve injury

Finally, all NRG1 isoforms, both soluble and transmembrane, can be classified as type a, b, or c isoforms, according to the exon present in the C-terminal part of the protein (Falls, 2003; Mei & Xiong, 2008).

A strong expression of the type a isoform is detectable at day-1 after injury (p<0.001) in all experimental models (crush: 7.92 ± 0.35 fold; end-to-end: 11.32 ± 0.47 fold; degenerating nerve: 13.85 ± 3.12 fold). From day-3 the expression returns to control values in the three experimental models, although under degenerating conditions this decrease is slower (at day-3: 1.76 ± 0.33 fold, p=0.070) (Figure 3).

The expression pattern of the type b NRG1 isoform is similar to type a, with a peak at day-1 from the injury (p<0.001) in three injury models (crush: 7.76 ± 1.83 fold; end-to-end: 11.33 ± 3.20 fold; degenerating nerve: 15.55 ± 3.09 fold). Under regenerating conditions the expression returns to control values from day-3 onward, whereas under degenerating conditions the expression is still high at day-3 (2.38 ± 0.31, p=0.011) (Figure 3).

Finally, the mRNA expression of the type c NRG1 isoform is strongly down-regulated after injury, remaining low until the end of the observation period (crush: 0.23 ±

0.12 fold, p=0.016; end-to-end: 0.05 ± 0.01 fold, p<0.001; degenerating nerve: 0.25 ± 0.02 fold, p=0.050) (Figure 3).

Statistical analysis revealed significant effects related to the type of injury for NRG1 type a, type b and type c, as shown in Figure 3.

NRG1/ErbB mRNA expression patterns depend on the expression by cells resident to the nerve

To investigate whether the deep changes observed at day-1 after injury are dependent on cells resident to the nerve or on cells invading it after injury, such as e.g. macrophages, healthy median nerve samples were put into degeneration *in vitro* for 1 day and the mRNA expression level was analysed and compared to fresh healthy control levels. As depicted in Figure 4, all analysed genes demonstrated an expression pattern similar to the expression pattern detected *in vivo* under degenerating conditions.

ErbB receptor protein expression is strongly up-regulated at day-7 after injury

The protein expression level of ErbB1, ErbB2 and ErbB3 receptors and of some NRG1 isoforms following nerve injury was assessed by western blot analysis of proteins obtained from the same samples analysed for mRNA expression levels.

ErbB1 protein (Figure 5) is expressed in the healthy control nerve and, following injury, its expression initially decreases. At day-3 after injury, however, protein expression is already increased and remains almost stably up-regulated until day-28 under regenerating conditions. Under degeneration conditions ErbB1 expression level demonstrated a constantly increasing up-regulation until the end of the observation period. Protein expression levels do not reflect the changes detected for mRNA expression levels (Figure 1). This is most evident under the degenerating conditions.

ErbB2 shows a protein expression pattern (Figure 5) which is again strongly different from the mRNA expression pattern (Figures 1): ErbB2 protein is barely detectable in healthy control nerve samples or until day-3 after injury, while its expression is strongly up-regulated at day-7 to day-14, followed by a slight decrease until day-28. ErbB2 protein expression levels are similar under regenerating and degenerating conditions, while mRNA expression is differentially regulated and never displaying an up-regulation.

ErbB3 protein (Figure 5) is expressed in healthy control nerve samples and strongly down-regulated until it is almost undetectable at day-3 after injury. At day-7, however, similar to ErbB2 protein, ErbB3 protein expression levels are strongly up-regulated and remain high 14 and 28 days after injury. The ErbB3 protein expression levels reflect the changes detected for ErbB3 mRNA expression (Figure 1).

The PI3K and the ERK MAP kinase pathways are activated following nerve injury

Two signal transduction pathways were analysed under regenerating and degenerating conditions: the phosphatydil-inositol-3 kinase (PI3K), and the ERK MAP kinase pathways.

A basal expression level of phosphorylated AKT phosphorylation is detectable in healthy nerve samples and an increased expression can be appreciated 7 days after injury in the end-to-end repaired and degenerating distal nerve samples. In Figure 5, the band corresponding to the phosphorylated AKT is detectable between two unspecific bands. Its identification was possible by comparison with the band corresponding to the total AKT protein.

Phosphorylated ERK 1/2 protein (Figure 5) is barely detectable in healthy nerve samples and strongly up-regulated at day-1 after injury where it remains high until day-7 prior to its slow decrease until day-28 after injury. At day-3 in the end-to-end group and at day-3 and day-7 in the degenerating nerve ERK seems less phosphorylated, but this is due to a lower amount of protein extract loaded for these samples, as can be verified from total ERK analysis.

Protein levels of different NRG1 isoforms are differentially regulated after injury

The analysis of NRG1 expression is a very difficult aim, both at mRNA and protein level, because several isoforms exist, which are characterized by the combination of exons shared in part with other isoforms (Figure 6). We analysed NRG1 expression using two specific antibodies: AB5551, directed to the cytoplasmic N-terminus shared by all transmembrane type III isoforms, and sc-348, directed to the type “a” cytoplasmic C-terminus. The “a” exon is one of the three possible known C-termini (which can be a, b, or c) downstream the transmembrane and the cytoplasmic domain common to all transmembrane NRG1 isoforms (soluble type I/II pro-proteins, transmembrane type III,

alpha, beta isoforms) except the β3 isoforms, which lack this region and are produced as “ready-to-use” proteins (Falls, 2003; Mei & Xiong, 2008).

In Figure 6A, the entire western blot for NRG1 proteins is shown, because the AB5551 antibody recognizes several bands which seem to be regulated following nerve injury. In particular, we focused on two bands.

The 100 kDa band, which seems to be expressed not only by axons but also by SC, appears between day-3 and day-7 after injury and its expression is switched off 28 days after injury under regenerating conditions while it remains highly expressed under degenerating conditions. This band seems to reflect the expression of a full length type III NRG1, isoform b or c, due to its high molecular weight. It is likely not reflecting expression of full length type III NRG1 isoform type “a”, because it is not detectable with the antibody sc-348 (Figure 6B).

With AB5551, another interesting band can be detected at approximately 75 kDa. The molecular weight of this band increases slightly after injury suggesting that this small increase could be due to a switch between ADAM17/TACE and BACE1 proteolytic cleavage of the detected type III NRG1. As illustrated in Figure 6C, when analysing type III NRG1 protein expression with an antibody recognizing the N-terminus of the protein, the product after cleavage by the α-secretase ADAM17/TACE (the α-N-terminal fragment/α-NTF), has a lower molecular weight than the product cleaved off by the β-secretase BACE1 cleavage, the β-NTF. On the contrary, when the expression of the type III NRG1 protein is analysed with an antibody recognizing the C-terminus of the protein, the product of the ADAM17/TACE cleavage (the α-C-terminal fragment/α-CTF) has a higher molecular weight than the product of the BACE1 cleavage (β-CTF), as previously elegantly shown by others (Fleck *et al.*, 2013).

Regarding the expression levels of the NRG1 α-NTF and β-NTF, the healthy nerve expresses only the α-NTF (Figure 6A).

Under regenerating conditions after mild injury (crush) both α-NTF and β-NTF are weakly expressed at day-1 and exclusively β-NTF at day-3. At day-7 and day-14 after injury α-NTF is strongly and β-NTF weakly expressed with the expression of the latter being eliminated at day-28 (resembling the status of a healthy nerve segment).

Under regenerating conditions after a more severe injury (end-to-end repair), α-NTF is still expressed in the distal nerve segment at day-1 after injury, then completely disappears until the end of the observation period (day-28), when it is expressed again

(resembling the expression pattern of a healthy nerve segment). At day-3 and day-7 after end-to-end repair the β-NTF band is only barely detectable in regenerating distal nerve segments, and its expression increases at day-14.

Under degenerating conditions, however, α-NTF expression disappears at day-1 after injury, while β-NTF is observed over the complete observation period, during which no regeneration occurs.

Lower molecular weight bands (around 50 kDa) were also detected, whose expression seems to increase after injury in the three experimental models.

The same nerve specimen, as subjected to AB5551 western blot analysis, were subjected to analysis with an antibody (sc-348) recognizing a 75k Da band corresponding to the C-terminal fragment (CTF) of type “a” NRG1 isoforms (Figure 6B). An expression increase of CTF was detectable after injury. This was followed by a decrease in protein levels under regenerating conditions (crush: at day-7; end-to-end: at day-28), while in the degenerating nerve the expression level remained stably elevated.

The CTF band detectable with sc-348 antibody does not show alpha and beta fragments like the NTF band, thus suggesting that this CTF derives mainly from the cleavage of type I/II NRG1 isoforms and not from type III NRG1 isoforms.

Distal nerve morphology displays different phases under regenerating and degenerating conditions

The ultrastructure of distal nerve segments was investigated by electron microscopy analysis (Figure 7). In particular, we focused on regenerating (crush) and degenerating nerves, assuming that end-to-end-repaired distal nerve morphology will resemble that of the crushed nerve just with a delay.

One day after injury (Figure 7, A, F), the general organization of the median nerve morphology is preserved under both regenerating and degenerating conditions and similar to that of a healthy control nerve, just some signs of fibre degeneration are already detectable, like e.g. partially de-compacted myelin sheaths surrounding collapsed axons.

Three days after injury (Figure 7, B, G), first signs of Wallerian degeneration are clearly detectable in both the regenerating and the degenerating condition. Nerve fascicles display dispersed fibres with an increased amount of connective tissue between them; some fibres show detachment and vacuolization of myelin lamellae, causing axolemma

exposure. However, many fibre profiles still present a normal ultrastructure in both crushed and degenerating nerves.

Seven days after injury (Figure 7, C, H), almost all nerve fibres display degeneration in both experimental groups. The nerve samples contain mainly collapsed axons with disintegrated myelin sheaths. Dedifferentiated SC with phagocytic properties are frequently detected by the numerous vacuoles in their cytoplasm.

Fourteen days after injury (Figure 7, D, I) first differences between the distal nerve segments under regenerating and degenerating conditions are evident. In the crushed nerve segments, first small diameter and thin myelinated axon profiles are detectable and indicate that the regeneration phase has been initiated between day 7 and 14 post injury. In contrast, distal segments under degenerating conditions display almost no more degenerating axons profiles, only few onion bulb like structures of degenerated myelinated axons are left. But also no regenerating axon profiles like in the crushed nerve are detectable.

Upon final analysis, 28 days after injury, (Figure 7, E, J), differences between the regenerating and degenerating nerve segments are preserved. In the crushed nerve not only the number of regenerating axon profiles is increased, but also the diameter and myelin sheath thickness of the regenerating axons. This is indicative for the phase of fibre maturation. In contrast, under degenerating condition, the phase of chronic denervation is reflected by the completed clearance of myelin and the presence of dedifferentiated SC with no more phagocytic properties.

MBP protein expression reflects different nerve regeneration stages

The analysis of the myelin basic protein (MBP) expression (Figure 8), both at mRNA and protein level, was utilized as a measure of myelination in distal nerve segments under regenerating and degenerating conditions.

MBP mRNA level (Figure 8A) strongly decreases ($p<0.001$) after injury demonstrating lowest expression levels from day-3 to day-7. This reflects the phase of Wallerian degeneration also detectable on a morphological level (Figure 7B, C, G, H). In the following, MBP mRNA levels are up-regulated towards healthy control nerve levels under regenerating conditions. Reflecting the phases of axonal regrowth and maturation which are again also detectable on a morphological level (Figure 7D), healthy control values are already almost reached at day-14 after injury in distal segments of crushed

nerves, while this is not detected before day-28 after end-to-end repair. The latter finding indicates that axonal regrowth and maturation as well as remyelination are delayed after end-to-end repair in comparison to crush injuries. Under degenerating conditions, however, MBP mRNA levels remain strongly down-regulated, reflecting the entry into the morphologically detectable phase of chronic denervation (Figure 7I, J).

MBP protein expression level (Figure 8B) again reflects the morphologically evident phases although its decrease demonstrates a lower kinetic. Under regenerating conditions at day-14, MBP protein is weakly expressed in distal segments of crushed nerves while the protein completely disappeared after end-to-end repair. In the following, the MBP protein expression level starts to recover towards healthy control nerve levels, displaying a delay after end-to-end repair compared to crush injury. Under degenerating conditions, MBP protein expression continuously disappeared from day-14 onward.

Discussion

As summarized in Figure 9, the components of the NRG1/ErbB system are differentially regulated during the time course of peripheral nerve regeneration and degeneration. In the current study, three experimental conditions have been investigated with crush injury and end-to-end repair reflecting two regenerating conditions which demonstrate all phases from Wallerian degeneration over axonal regrowth to axonal maturation and remyelination following a different time course. In contrast, the unrepaired nerve reflected the degeneration condition represented by complete removal of peripheral myelin on morphological and protein level and no signs of axonal regrowth or remyelination in the chronic denervation phase. Differential regulation of the NRG1/ErbB system components on mRNA and protein levels can be specifically linked to the different phases of biomolecular and morphological changes the distal nerve segments undergo under regenerating and degenerating conditions.

The NRG1/ErbB system is deeply involved in peripheral nerve myelination and remyelination processes and several previous studies by others and us focused on the role of soluble and transmembrane NRG1 isoforms in these late phases of nerve regeneration (Fricker & Bennett, 2011; Gambarotta *et al.*, 2013). In particular, it has been shown that transmembrane type III NRG1 plays a key role both in myelination and remyelination (Michailov *et al.*, 2004; Taveggia *et al.*, 2005; Fricker *et al.*, 2011; Stassart *et al.*, 2013), while it has been suggested that soluble type I/II NRG1 is mainly involved in SC survival, redifferentiation and, therefore, in remyelination (Stassart *et al.*, 2013).

To our knowledge, this is the first time that mRNA expression levels also in the early phases after peripheral nerve injury were discriminated between not only soluble and transmembrane isoforms - which are involved in autocrine/paracrine and juxtacrine interactions - but also between type alpha and type beta isoforms - which are characterized by different activity - and between type a, type b and type c isoforms - which differ for the cytoplasmic C-terminal domain involved in NRG1 back signalling.

We demonstrate here that NRG1 isoforms are differentially regulated after nerve injury, where we detected a strong increase of mRNA of the NRG1 type I/II, alpha and beta, as well as type a and type b at day-1. Therefore, we hypothesize that the observed NRG1 expression peak corresponds to different combinations of NRG1 type I/II, alpha and beta, a and b. A strong increase of soluble NRG1 expression at day-1 after nerve injury

was already described (Stassart *et al.*, 2013) as well as the up-regulation of NRG1 alpha by others and us (Carroll *et al.*, 1997; Nicolino *et al.*, 2003).

Alpha and beta NRG1 isoforms are known to differ in their activity, with alpha isoforms being about 10 fold less active than beta isoforms (Pinkas-Kramarski *et al.*, 1996). However, the difference between alpha and beta isoforms seems to be not only quantitative, but also qualitative. Indeed, it has been shown that NRG1 alpha and beta differentially affect the migration and invasion of malignant peripheral nerve sheath tumor cells (Eckert *et al.*, 2009) and that NRG1 alpha is able to regulate genes involved in phosphorylation, acetylation and alternative splicing in lymphoblastoid cells (Ghahramani-Seno *et al.*, 2013). The concomitant up-regulation of both the NRG1 alpha and beta isoforms demonstrated in this study indicates that both play a regulatory role following peripheral nerve injury.

The C-terminal domain of NRG1 (which can be type a, type b or type c) is a domain common to all soluble and transmembrane NRG1 isoforms, except NRG1 β3, and it is involved in the back signalling mediated by transmembrane NRG1 isoforms following interaction with ErbB receptors. Indeed, it has been demonstrated that, following NRG1/ErbB interaction, a γ-secretase cleavage releases a NRG1 intracellular domain (ICD) that translocates into the nucleus and, according to the cell model analysed, represses the expression of genes regulating apoptosis (Bao *et al.*, 2003), up-regulates the expression of postsynaptic density protein-95 (PSD-95) (Bao *et al.*, 2004) and the expression of prostaglandin D2 synthase (L-PGDS) which, together with the G protein–coupled receptor Gpr44, is involved in peripheral nerve myelination (Trimarco *et al.*, 2014). We observed here a transient up-regulation of NRG1 isoforms containing type a and type b C-terminal ends, whereas the type c isoforms stably decrease after nerve injury. Further studies are necessary to investigate the role of type a, b, and c NRG1 isoforms both during development of the peripheral nervous system and after nerve injury.

At the protein level, we analysed NRG1 expression using two antibodies, one directed to the cytoplasmic N-terminus common to all transmembrane type III NRG1, and one directed to the type a NRG1 C-terminus which can be present both in transmembrane type III NRG1 and in the transmembrane precursors of soluble type I/II NRG1. The most interesting data were obtained with the first antibody.

After peripheral nerve injury we observed a “switch on” of a 100 kDa band, expressed also by SC, and a “switch-off” of the same 28 days after injury under

regenerating conditions, while it remained to be expressed in the degenerating condition, as previously described (Carroll *et al.*, 1997). The high molecular weight of the band suggests that it is a full length type III NRG1, isoform b or c (not a, because the antibody directed to the type a domain did not detect it). The protein expression pattern suggests that this isoform plays a crucial role for nerve regeneration.

Transmembrane NRG1 is usually considered to be expressed by axons and we demonstrate in this study that this expression is related to the phase of axonal regrowth. Nevertheless, its strong and stable expression observed also in the degenerating nerve and in SC suggests that this transmembrane isoform is of glial origin or potentially translated in the axon from previously transcribed mRNA. The latter hypothesis can be concluded from our NRG1 type III mRNA analysis that is not changed under regenerating conditions, while slightly increased (with a high standard error) in the degenerating nerve.

Intriguingly, we observed the presence of a band with a molecular weight around 75 kDa, whose weight slightly increases after injury. We hypothesized that this small increase could be due to a switch between ADAM17/TACE to BACE1 proteolytic cleavage of type III NRG1.

It has been previously shown by others that products resulting from ADAM17/TACE cleavage of type III NRG1 inhibit remyelination (La Marca *et al.*, 2011), while products resulting from BACE1 cleavage promote myelination (Willem *et al.*, 2006). On the other hand, it has recently been shown that products resulting from BACE1 cleavage are not essential for the activation of myelination probably because additional proteases can also process NRG1 type III (Velanac *et al.*, 2012).

To our knowledge, the data in this study evidence, for the first time, a switch between the two cleavage activities of ADAM17/TACE and BACE1 following peripheral nerve injury *in vivo.* Our data show that the healthy nerve expresses only the α-N-terminal-Fragment (α-NTF) of NRG1, which is the product of ADAM17/TACE cleavage, while regenerating nerves after end-to-end repair express only β-NTF, the product of the BACE1 cleavage which promotes remyelination. In contrast, regenerating nerves after a milder injury (crush) express both α-NTF and β-NTF of NRG1, suggesting that in this model axonal regrowth and remyelination phases are partially overlapping. Finally, 4-weeks after injury regenerating nerves express only α-NTF, indicating that remyelination is completed at that time after a crush injury as well as after end-to-end repair. Under degenerating

conditions β-NTF is still expressed 28 days after injury, indicating that the machinery is kept on “stand-by” for eventually still regrowing axons.

As after axonotmesis (crush) and neurotmesis (transection and repair or non-repaired), the continuity between distal axons and the corresponding cell bodies is disrupted, it is very likely that the NRG1 β-NTF band we observe after nerve injury is locally synthesized in the analysed nerve segments. This hypothesis is strengthened by data demonstrating that peripheral nerves contain mRNA, ribosomal proteins and Golgi-like structures and that local translation can occur in the injured nerve (Yoo *et al.*, 2010). Intriguingly, intercellular transport of ribosomes (Court *et al.*, 2011) and mRNA (Giuditta *et al.*, 2002; Sotelo *et al.*, 2014) from SC to axons has been demonstrated before. The latter reinforces the idea that SC may support local axonal protein synthesis.

In order to assign the 75 kDa C-terminal fragment (CTF) band to specific NRG1 isoforms, the following conclusions can be drawn from our data. NRG1 protein expression levels were analysed with one antibody directed against the cytoplasmic NRG1 C-terminus which is shared by all isoforms containing the exon defining type a isoforms. Therefore, the 75 kDa CTF can derive either from the proteolytic cleavage of the transmembrane type III NRG1 isoforms or the proteolytic cleavage of the pro-protein type I/II isoforms (which are transmembrane, but release an extracellular soluble fragment, leaving a membrane anchored C-terminus).

However, because we observed two different molecular weights for the N-terminal fragment of NRG1 with the AB5551 antibody directed to the type III NRG1 (α-NTF and β-NTF), and only a single band with the sc-348 antibody directed to the C-terminal fragments of NRG1 (α-CTF and β-CTF) we hypothesize that this band corresponds to the CTF derived from the proteolytic cleavage of the precursor of type I/II NRG1 type a isoform. The two bands of type III NRG1 isoforms observed with the AB5551 antibody must then represent type b or type c isoforms.

With regard to the NRG1 signalling after peripheral nerve injury, we also analysed the expression of ErbB receptors again both at mRNA and protein level.

Under regenerating conditions ErbB2 and ErbB3 mRNA levels show a down-regulation at day-1 after injury, followed by a strong up-regulation of ErbB3 while ErbB2 mRNA level decreases to constant low levels. At the protein level, the regenerating condition is reflected by an initial decrease of ErbB1 and ErbB3 protein followed by a strong up-regulation of ErbB1-3. Until the end of the observation period, ErbB1 and ErbB2

proteins are down-regulated again in the regenerating nerve samples at day-28 after injury, although their expression is still higher than control.

Under degenerating conditions, ErbB1 and ErbB2 mRNA expression is constantly comparable to the control during all time points analysed, while the initially down-regulated ErbB3 mRNA level increases at day-7 after injury and remains highly up-regulated until day-28. At the protein level, ErbB1 expression is constantly increased under degenerating conditions, while the protein expression patterns of ErbB2 and ErbB3 are similar those under regenerating conditions. Our data obtained in the degenerating nerve are consistent with a previous study of ErbB and NRG1 expression during Wallerian degeneration after sciatic nerve transection injury (Carroll *et al.*, 1997).

The strong up-regulation of ErbB2 protein in the early phase after injury is independent of the repair conditions provided and does not correspond to an mRNA expression level increase. We confirm, however, that the ErbB2 transcript level is stably high in the analysis of the threshold cycle by real time PCR. Therefore, it is very likely that the strong protein up-regulation after nerve injury is the consequence of post-transcriptional regulation occurring through different signal transduction pathways. Indeed, different research groups analysed already the expression of microRNAs and their role in post-transcriptional regulation following nerve injury (Viader *et al.*, 2011; Wu *et al.*, 2011; Chang *et al.*, 2013; Nagata *et al.*, 2014; Zhou *et al.*, 2014). And, the injury induced down-regulation of microRNAs having ErbB2 and ErbB3 as target genes could contribute to ErbB2 and ErbB3 protein up-regulation (Scott *et al.*, 2007). Moreover, post-transcriptional regulation could be the consequence of protein kinase A (PKA) activation occurring after nerve injury. Related to this hypothesis, it has been demonstrated *in vitro* that NRG1 and forskolin synergize and that forskolin increases ErbB2-ErbB3 protein expression in human SC without increasing levels of mRNA encoding these receptors (Fregien *et al.*, 2005). Forskolin activates the enzyme adenylyl cyclase thus increasing intracellular levels of cyclic adenosine monophosphate (cAMP), an important second messenger that acts by activating cAMP-sensitive pathways such as PKA. Therefore, the activation of cAMP signalling, which has also been shown to synergize with NRG1 in the promotion of myelination (Arthur-Farraj *et al.*, 2011), could contribute to ErbB2 protein up-regulation.

The regulation of NRG1 and ErbB mRNA expression we observed in the degenerating nerve *in vivo* was confirmed also *in vitro*, suggesting that the corresponding genes are expressed by cells resident inside the nerve.

Finally, we analysed AKT and ERK phosphorylation to investigate the existence of possible differences in the signal transduction pathways activated in response to the regenerating or degenerating conditions after peripheral nerve injury. AKT is more phosphorylated in the end-to-end repaired and degenerating samples, suggesting that it is involved in the response to more severe injuries. ERK signalling was already described before to be rapidly and strongly activated following nerve injury (Sheu *et al.*, 2000; Harrisingh *et al.*, 2004; Napoli *et al.*, 2012). Our data obtained from the current study, however, do not display any differences among the regenerating and degenerating conditions during the observation period. With high levels of phosphorylated ERK at day-1 after injury and its disappearance at day-28 it is likely that the role of ERK is more linked to the general response of the nerve after injury than to regeneration or degeneration.

Conclusion

We demonstrate here that the components of the NRG1/ErbB system are differently regulated in the different phases a peripheral nerve undergoes after injury with the aim to regenerate. The immediate response to nerve injury is represented by ERK phosphorylation and by the up-regulation of soluble NRG1 (type alpha and beta, type a and b), which suggests that soluble NRG1 isoforms are involved in the response to nerve injury, stimulating SC survival and promoting axon regrowth. One week after injury, expression of ErbB2/ErbB3 co-receptor also is strongly up-regulated.

We additionally identified a highly expressed type III NRG1 100 kDa isoform, the expression of which is only switched off after axon regeneration.

Furthermore, our data suggest the existence of a reversible switch between ADAM17/TACE and BACE1 cleavage activity of type III NRG1 following nerve injury, which is very likely needed for the regulation of the remyelination process.

Moreover, we demonstrate here for the first time the involvement of type a, b and c isoforms in peripheral nerve regeneration. Further studies will be necessary to better understand their role in the back signalling mediated by NRG1.

The precise regulation of the components of the NRG1/ErbB system indicates that each molecule that undergoes changes on the mRNA and protein level is crucially involved in successful peripheral nerve regeneration and could be a target for pre-clinical evaluation of regeneration promoting factors.

Acknowledgements

This project has received funding from the European Union's Seventh Programme for research, technological development and demonstration under grant agreement No [278612]. The authors declare that no conflict of interest exist.

Abbreviations

A disintegrin and metalloprotease (ADAM17)
Cyclic adenosine monophosphate (cAMP)
β-site of amyloid precursor protein-cleaving enzyme1 (BACE1)
C-terminal fragment (CTF)
Dulbecco's Modified Eagle Medium (DMEM)
Epidermal Growth Factor (EGF)
Foetal bovine serum (FBS)
Intracellular domain (ICD)
Lipocalin-type prostaglandin D2 synthase (L-PGDS)
Myelin basic protein (MBP)
Neuregulin1 (NRG1)
N-terminal fragment (NTF)
Peripheral Nervous System (PNS)
Phosphatydil-inositol-3 kinase (PI3K)
Protein kinase A (PKA)
Schwann cells (SC)
Tumour necrosis factor-α-converting enzyme (TACE)

Figure legends

Table I: Primers used for quantitative real time PCR analysis. The name of the amplified gene or isoform is indicated in the first column, followed by the accession number to reference sequences. The primer name indicates if the primers anneals only to *Rattus norvegicus* sequences (r) or also to *Mus musculus* (m).

Figure 1: ErbB mRNA is highly regulated after nerve injury. The relative quantification (-ΔΔCt) of ErbB1, ErbB2 and ErbB3 receptor was obtained by quantitative real-time PCR: data were normalized to the geometric mean of two endogenous housekeeping genes (ANKRD27 and RICTOR). Values in the graphics are expressed as mean ± SEM. Statistical analysis (one-way ANOVA with Bonferroni's post hoc) was carried out to compare the differences among the three injury models at each time point. Asterisks (*) denote statistically significant differences between crush and end-to-end repair conditions; dollars ($) between crush and degenerating nerves conditions; hashes (#) between end-to-end repair and degenerating nerve conditions (*/$/#: $p \leq 0.05$, **/$$/##: $p \leq 0.01$ and ***/$$$/###: $p \leq 0.001$). Statistical analysis of the comparison of each time point with control condition is discussed in the text.

Figure 2: **NRG1 soluble isoforms are strongly up-regulated at mRNA level immediately after nerve injury.** The relative quantification (-ΔΔCt) of NRG1 type I/II, NRG1 type III, NRG1α and NRG1β was obtained by quantitative real-time PCR: data were normalized to the geometric mean of two endogenous housekeeping genes (ANKRD27 and RICTOR). Values in the graphics are expressed as mean ± SEM. Statistical analysis (one-way ANOVA with Bonferroni's post hoc) was carried out to compare the differences among the three injury models at each time point. Asterisks (*) denote statistically significant differences between crush and end-to-end repair conditions; dollars ($) between crush and degenerating nerves conditions; hashes (#) between end-to-end repair and degenerating nerve conditions (*/$/#: $p \leq 0.05$, **/$$/##: $p \leq 0.01$ and ***/$$$/###: $p \leq 0.001$). Statistical analysis of the comparison of each time point with control condition is discussed in the text.

Figure 3: NRG1 type a and type b isoforms are up-regulated at mRNA level after nerve injury. The relative quantification (-ΔΔCt) of NRG1 type a, type b and type c was obtained by quantitative real-time PCR: data were normalized to the geometric mean of two endogenous housekeeping genes (ANKRD27 and RICTOR). Values in the graphics are expressed as mean ± SEM. Statistical analysis (one-way ANOVA with Bonferroni's post hoc) was carried out to compare the differences among the three injury models at each time point. Asterisks (*) denote statistically significant differences between crush and end-to-end repair conditions; dollars ($) between crush and degenerating nerves conditions; hashes (#) between end-to-end repair and degenerating nerve conditions (*/$/#: $p \leq 0.05$, **/$$/##: $p \leq 0.01$ and ***/$$$/###: $p \leq 0.001$). Statistical analysis of the comparison of each time point with control condition is discussed in the text.

Figure 4: NRG1/ErbB expression in *in vitro* degenerating nerves. Nerves were cultured for 1 day. This *in vitro* experimental procedure mimics *in vivo* nerve degeneration. The relative quantification (-ΔΔCt) of NRG1/ErbB was obtained by quantitative real-time PCR: data were normalized to the geometric mean of two endogenous housekeeping genes (ANKRD27 and RICTOR). Values in the graphics are expressed as mean + SEM. One-way ANOVA with Bonferroni's post hoc was used for statistical analysis (*: $p \leq 0.05$, **: $p \leq 0.01$ and ***: $p \leq 0.001$).

Figure 5: **ErbB receptor proteins are deeply regulated in the three experimental injury models**. Western blot analysis of proteins extracted from healthy nerves (0) and distal segments of injured nerves at different time points, separated on 8% gels (50 µg/ lane) and probed with antibodies for ErbB1, ErbB2, ErbB3, p-AKT, total-AKT, p-ERK, total-ERK, MBP, GAPDH, β-actin. The same samples were run on three independent gels to analyse the expression of different proteins characterized by the same molecular weight. The positions of the detected proteins is indicated on the left, size markers on the right.
The band corresponding to the phosphorylated AKT is detectable between two unspecific bands. Its identification was possible by comparison with the band corresponding to the total AKT protein.

Figure 6: **NRG1 isoforms are deeply regulated at protein level in the three experimental injury models.** Western blot analysis of proteins extracted from healthy nerves (0) and from the distal segment of injured nerves at different time points. Proteins (50 µg/lane) were separated on 4-15% gels. In the panel A proteins were probed with an antibody (AB5551) directed to the N-terminus of all type III NRG1 isoforms. This antibody recognizes: a 100 kDa band (detected also in adult primary Schwann cells-SC) whose expression switch on after injury and off after regeneration, but remains on in the degenerating nerve; a pair of bands about 75 kDa which would correspond to the N-terminus fragments (NTF) resulting from α (ADAM17/TACE) or β (BACE) secretase cleavage of type III NRG1 (α–NTF, β-NTF); some bands around 50kDa, whose expression seems to be regulated following injury, but whose identity is currently unclear. In the panel B the same samples were probed with an antibody (sc348) directed to the type a C-terminus common to many NRG1 isoforms. This antibody recognizes only a 75 kDa band which would correspond to the C-terminus fragment (CTF) resulting from the cleavage of type a NRG1 isoforms (both soluble and transmembrane). The positions of the detected proteins is indicated on the left, size markers are indicated on the right. In the panel C a very simplified structure of type I/II soluble isoforms and type III transmembrane isoforms of NRG1 is schematized, together with antibody epitope. This scheme illustrates that type I/II and type III isoforms differ for the N-terminus regions, that the CTF can derive from both type I/II and type III NRG1 isoform cleavage, and that CTF can be recognized by sc-348 only if its C-terminal end is type a. ADAM17/TACE and BACE1 cleavage sites on type III NRG1 are shown, to illustrate how the NTF fragment produced by the BACE1 cleavage (β-NTF) has a molecular weight higher than the NTF fragment produced by the ADAM17/TACE (α–NTF) cleavage.

Figure 7: Representative electron micrographs of transverse median nerve sections of crushed nerve (A;B;C;D;E) and degenerating nerve (F;G;H;I;J) after 1 day (A;F), 3 days (B;G), 7 days (C;H), 14 days (D;I) and 28 days (E;J) from the injury. 1 day, 3 days and 7 days after injury, nerve morphology appears similar in both experimental models: 1 day after injury (A,F), partially de-compacted myelin sheaths (white asterisks) are visible; after 3 days (B,G), increasing amount of connective tissue can be appreciated, as well as detached myelin lamellae (white asterisks). 7 days after injury (C, H), almost all nerve fibres display degeneration: collapsed axon with disintegrated myelin sheath (white

asterisks) and the dedifferentiated SC with phagocytotic properties (white arrow head) are detected. 15 days after injury, differences between regenerating and degenerating nerves are evident: in the crushed nerve (D) small diameter regenerating axons with thin myelin (some fibres are indicated with black asterisks in the figure) are detected, whereas under degenerating condition (I) onion bulbs can be still seen (white asterisks). Finally, after 28 days, regenerating axon profiles with increased diameter and myelin sheaths are detected in crush injury group (E), while under degenerating conditions, dedifferentiated SC without vacuoles are present in the nerve distal segment (white asterisks, J). Scale bar: 5 μm

Figure 8: MBP expression reflects the nerves regenerating and degenerating conditions. The relative quantification (-ΔΔCt) of MBP (A) was obtained by quantitative real-time PCR: data were normalized to the geometric mean of two endogenous housekeeping genes (ANKRD27 and RICTOR). Values in the graphics are expressed as mean ± SEM. One-way ANOVA was used for statistical analysis with */$/#: $p \leq 0.05$, **/$$/##: $p \leq 0.01$ and ***/$$$/###: $p \leq 0.001$ in order to compare the differences among the three model of injury at each time point. Asterisks (*) denote statistically significant differences between crush and end-to-end repair conditions; dollars ($) between crush and degenerating nerve conditions; hashes (#) between end-to-end repair and degenerating nerve conditions (*/$/#: $p \leq 0.05$, **/$$/##: $p \leq 0.01$ and ***/$$$/###: $p \leq 0.001$). Statistical analysis of the comparison of each time point with control condition is discussed in the text. Western blot analysis (B) showing MBP expression in the three injury models. β-actin and GAPDH were used as a loading control.

Figure 9: **Schematic representation of all mRNA and protein data shown in this paper.** Upward and downward arrows represent up-regulation and down-regulation respectively. This graphical representation is not intended to exactly indicate the beginning and the ending of the three phases occurring after nerve injury (nerve degeneration, axon growth and remyelination), but rather the period when each process mainly occurs.

References

Adlkofer, K. & Lai, C. (2000) Role of neuregulins in glial cell development. *Glia*, **29**, 104-111.

Arthur-Farraj, P., Wanek, K., Hantke, J., Davis, C.M., Jayakar, A., Parkinson, D.B., Mirsky, R. & Jessen, K.R. (2011) Mouse schwann cells need both NRG1 and cyclic AMP to myelinate. *Glia*, **59**, 720-733.

Bao, J., Lin, H., Ouyang, Y., Lei, D., Osman, A., Kim, T.W., Mei, L., Dai, P., Ohlemiller, K.K. & Ambron, R.T. (2004) Activity-dependent transcription regulation of PSD-95 by neuregulin-1 and Eos. *Nat Neurosci*, **7**, 1250-1258.

Bao, J., Wolpowitz, D., Role, L.W. & Talmage, D.A. (2003) Back signaling by the Nrg-1 intracellular domain. *J Cell Biol*, **161**, 1133-1141.

Carroll, S.L., Miller, M.L., Frohnert, P.W., Kim, S.S. & Corbett, J.A. (1997) Expression of neuregulins and their putative receptors, ErbB2 and ErbB3, is induced during Wallerian degeneration. *J Neurosci*, **17**, 1642-1659.

Chang, L.-W., Viader, A., Varghese, N., Payton, J.E., Milbrandt, J. & Nagarajan, R. (2013) An integrated approach to characterize transcription factor and microRNA regulatory networks involved in Schwann cell response to peripheral nerve injury. *BMC Genomics*, **14**, 84-103.

Court, F.A., Midha, R., Cisterna, B.A., Grochmal, J., Shakhbazau, A., Hendriks, W.T. & Van Minnen, J. (2011) Morphological evidence for a transport of ribosomes from Schwann cells to regenerating axons. *Glia*, **59**, 1529-1539.

Eckert, J.M., Byer, S.J., Clodfelder-Miller, B.J. & Carroll, S.L. (2009) Neuregulin-1 beta and neuregulin-1 alpha differentially affect the migration and invasion of malignant peripheral nerve sheath tumor cells. *Glia*, **57**, 1501-1520.

Falls, D.L. (2003) Neuregulins: functions, forms, and signaling strategies. *Exp. Cell Res.*, **284**, 14-30.

Fleck, D., van Bebber, F., Colombo, A., Galante, C., Schwenk, B.M., Rabe, L., Hampel, H., Novak, B., Kremmer, E., Tahirovic, S., Edbauer, D., Lichtenthaler, S.F., Schmid, B., Willem, M. & Haass, C. (2013) Dual cleavage of neuregulin 1 type III by BACE1 and ADAM17 liberates its EGF-like domain and allows paracrine signaling. *J Neurosci*, **33**, 7856-7869.

Fregien, N.L., White, L.A., Bunge, M.B. & Wood, P.M. (2005) Forskolin increases neuregulin receptors in human Schwann cells without increasing receptor mRNA. *Glia*, **49**, 24-35.

Fricker, F.R. & Bennett, D.L. (2011) The role of neuregulin-1 in the response to nerve injury. *Future Neurol*, **6**, 809-822.

Fricker, F.R., Lago, N., Balarajah, S., Tsantoulas, C., Tanna, S., Zhu, N., Fageiry, S.K., Jenkins, M., Garratt, A.N., Birchmeier, C. & Bennett, D.L. (2011) Axonally derived neuregulin-1 is required for remyelination and regeneration after nerve injury in adulthood. *J. Neurosci.*, **31**, 3225-3233.

Gambarotta, G., Fregnan, F., Gnavi, S. & Perroteau, I. (2013) Neuregulin 1 role in Schwann cell regulation and potential applications to promote peripheral nerve regeneration. *Int Rev Neurobiol*, **108**, 223-256.

Gambarotta, G., Garzotto, D., Destro, E., Mautino, B., Giampietro, C., Cutrupi, S., Dati, C., Cattaneo, E., Fasolo, A. & Perroteau, I. (2004) ErbB4 expression in neural progenitor cells (ST14A) is necessary to mediate neuregulin-1beta1-induced migration. *J Biol Chem*, **279**, 48808-48816.

Gambarotta, G., Ronchi, G., Friard, O., Iannello, A., Galletta, P. & Geuna, S. (2014a) Identification and validation of optimal reference genes to quantify gene expression following peripheral nerve injury. *PLoS One*, **9**, e105601.

Gambarotta, G., Ronchi, G., Geuna, S. & Perroteau, I. (2014b) Neuregulin 1 isoforms could be an effective therapeutic candidate to promote peripheral nerve regeneration. *Neural Regen Res*, **9**, 1183-1185.

Garratt, A.N., Voiculescu, O., Topilko, P., Charnay, P. & Birchmeier, C. (2000) A dual role of erbB2 in myelination and in expansion of the schwann cell precursor pool. *J. Cell. Biol.*, **148**, 1035-1046.

Ghahramani-Seno, M.M., Gwadry, F.G., Hu, P. & Scherer, S.W. (2013) Neuregulin 1-alpha regulates phosphorylation, acetylation, and alternative splicing in lymphoblastoid cells. *Genome*, **56**, 619-625.

Giuditta, A., Eyman, M. & Kaplan, B.B. (2002) Gene expression in the squid giant axon: neurotransmitter modulation of RNA transfer from periaxonal glia to the axon. *Biol Bull*, **203**, 189-190.

Gnavi, S., Fornasari, B.E., Tonda-Turo, C., Ciardelli, G., Zanetti, M., Geuna, S. & Perroteau, I. (2015) The influence of electrospun fibre size on Schwann cell behaviour and axonal outgrowth. *Mater Sci Eng C Mater Biol Appl*, **48**, 620-631.

Harrisingh, M.C., Perez-Nadales, E., Parkinson, D.B., Malcolm, D.S., Mudge, A.W. & Lloyd, A.C. (2004) The Ras/Raf/ERK signalling pathway drives Schwann cell dedifferentiation. *EMBO J*, **23**, 3061-3071.

Heermann, S. & Schwab, M.H. (2013) Molecular control of Schwann cell migration along peripheral axons: keep moving! *Cell Adh Migr*, **7**, 18-22.

La Marca, R., Cerri, F., Horiuchi, K., Bachi, A., Feltri, M.L., Wrabetz, L., Blobel, C.P., Quattrini, A., Salzer, J.L. & Taveggia, C. (2011) TACE (ADAM17) inhibits Schwann cell myelination. *Nat Neurosci*, **14**, 857-865.

Mei, L. & Xiong, W.C. (2008) Neuregulin 1 in neural development, synaptic plasticity and schizophrenia. *Nat. Rev. Neurosci.*, **9**, 437-452.

Michailov, G.V., Sereda, M.W., Brinkmann, B.G., Fischer, T.M., Haug, B., Birchmeier, C., Role, L., Lai, C., Schwab, M.H. & Nave, K.A. (2004) Axonal neuregulin-1 regulates myelin sheath thickness. *Science*, **304**, 700-703.

Nagata, K., Hama, I., Kiryu-Seo, S. & Kiyama, H. (2014) microRNA-124 is down regulated in nerve-injured motor neurons and it potentially targets mRNAs for KLF6 and STAT3. *Neuroscience*, **256**, 426-432.

Napoli, I., Noon, L.A., Ribeiro, S., Kerai, A.P., Parrinello, S., Rosenberg, L.H., Collins, M.J., Harrisingh, M.C., White, I.J., Woodhoo, A. & Lloyd, A.C. (2012) A central role for the ERK-signaling pathway in controlling Schwann cell plasticity and peripheral nerve regeneration in vivo. *Neuron*, **73**, 729-742.

Nicolino, S., Raimondo, S., Tos, P., Battiston, B., Fornaro, M., Geuna, S. & Perroteau, I. (2003) Expression of alpha2a-2b neuregulin-1 is associated with early peripheral nerve repair along muscle-enriched tubes. *Neuroreport*, **14**, 1541-1545.

Pereira, J.A., Lebrun-Julien, F. & Suter, U. (2012) Molecular mechanisms regulating myelination in the peripheral nervous system. *Trends Neurosci*, **35**, 123-134.

Pinkas-Kramarski, R., Shelly, M., Glathe, S., Ratzkin, B.J. & Yarden, Y. (1996) Neu differentiation factor/neuregulin isoforms activate distinct receptor combinations. *J Biol Chem*, **271**, 19029-19032.

Ronchi, G., Nicolino, S., Raimondo, S., Tos, P., Battiston, B., Papalia, I., Varejao, A.S., Giacobini-Robecchi, M.G., Perroteau, I. & Geuna, S. (2009) Functional and morphological assessment of a standardized crush injury of the rat median nerve. *J. Neurosci. Methods.*, **179**, 51-57.

Salzer, J.L. (2012) Axonal regulation of Schwann cell ensheathment and myelination. *J Peripher Nerv Syst*, **17 Suppl 3**, 14-19.

Scott, G.K., Goga, A., Bhaumik, D., Berger, C.E., Sullivan, C.S. & Benz, C.C. (2007) Coordinate suppression of ERBB2 and ERBB3 by enforced expression of micro-RNA miR-125a or miR-125b. *J Biol Chem* **282**, 1479-1486.

Sheu, J.Y., Kulhanek, D.J. & Eckenstein, F.P. (2000) Differential patterns of ERK and STAT3 phosphorylation after sciatic nerve transection in the rat. *Exp Neurol*, **166**, 392-402.

Sotelo, J.R., Canclini, L., Kun, A., Sotelo-Silveira, J.R., Calliari, A., Cal, K., Bresque, M., Dipaolo, A., Farias, J. & Mercer, J.A. (2014) Glia to axon RNA transfer. *Dev Neurobiol*, **74**, 292-302.

Stassart, R.M., Fledrich, R., Velanac, V., Brinkmann, B.G., Schwab, M.H., Meijer, D., Sereda, M.W. & Nave, K.A. (2013) A role for Schwann cell-derived neuregulin-1 in remyelination. *Nat Neurosci*, **16**, 48-54.

Taveggia, C., Feltri, M.L. & Wrabetz, L. (2010) Signals to promote myelin formation and repair. *Nat Rev Neurol*, **6**, 276-287.

Taveggia, C., Zanazzi, G., Petrylak, A., Yano, H., Rosenbluth, J., Einheber, S., Xu, X., Esper, R.M., Loeb, J.A., Shrager, P., Chao, M.V., Falls, D.L., Role, L. & Salzer, J.L. (2005) Neuregulin-1 type III determines the ensheathment fate of axons. *Neuron*, **47**, 681-694.

Trimarco, A., Forese, M.G., Alfieri, V., Lucente, A., Brambilla, P., Dina, G., Pieragostino, D., Sacchetta, P., Urade, Y., Boizet-Bonhoure, B., Martinelli Boneschi, F., Quattrini, A. & Taveggia, C. (2014) Prostaglandin D2 synthase/GPR44: a signaling axis in PNS myelination. *Nat Neurosci*, **17**, 1682-1692.

Velanac, V., Unterbarnscheidt, T., Hinrichs, W., Gummert, M.N., Fischer, T.M., Rossner, M.J., Trimarco, A., Brivio, V., Taveggia, C., Willem, M., Haass, C., Mobius, W., Nave, K.A. & Schwab, M.H. (2012) Bace1 processing of NRG1 type III produces a myelin-inducing signal but is not essential for the stimulation of myelination. *Glia*, **60**, 203-217.

Viader, A., Chang, L.-W., Fahrner, T., Nagarajan, R. & Milbrandt, J. (2011) MicroRNAs modulate Schwann cell response to nerve injury by reinforcing transcriptional silencing of dedifferentiation-related genes. *J Neurosci*, **31**, 17358-17369.

Willem, M., Garratt, A.N., Novak, B., Citron, M., Kaufmann, S., Rittger, A., DeStrooper, B., Saftig, P., Birchmeier, C. & Haass, C. (2006) Control of peripheral nerve myelination by the beta-secretase BACE1. *Science*, **314**, 664-666.

Wu, D., Raafat, M., Pak, E., Hammond, S. & Murashov, A. (2011) MicroRNA machinery responds to peripheral nerve lesion in an injury-regulated pattern. *Neuroscience*, **190**, 386-397.

Yarden, Y. & Sliwkowski, M.X. (2001) Untangling the ErbB signalling network. *Nat. Rev. Mol. Cell Biol.*, **2**, 127-137.

Yoo, S., van Niekerk, E.A., Merianda, T.T. & Twiss, J.L. (2010) Dynamics of axonal mRNA transport and implications for peripheral nerve regeneration. *Exp Neurol*, **223**, 19-27.

Zhou, S., Gao, R., Hu, W., Qian, T., Wang, N., Ding, G., Ding, F., Yu, B. & Gu, X. (2014) MiR-9 inhibits Schwann cell migration by targeting Cthrc1 following sciatic nerve injury. *J Cell Sci.* , **127**, 967-976.

Figure 1

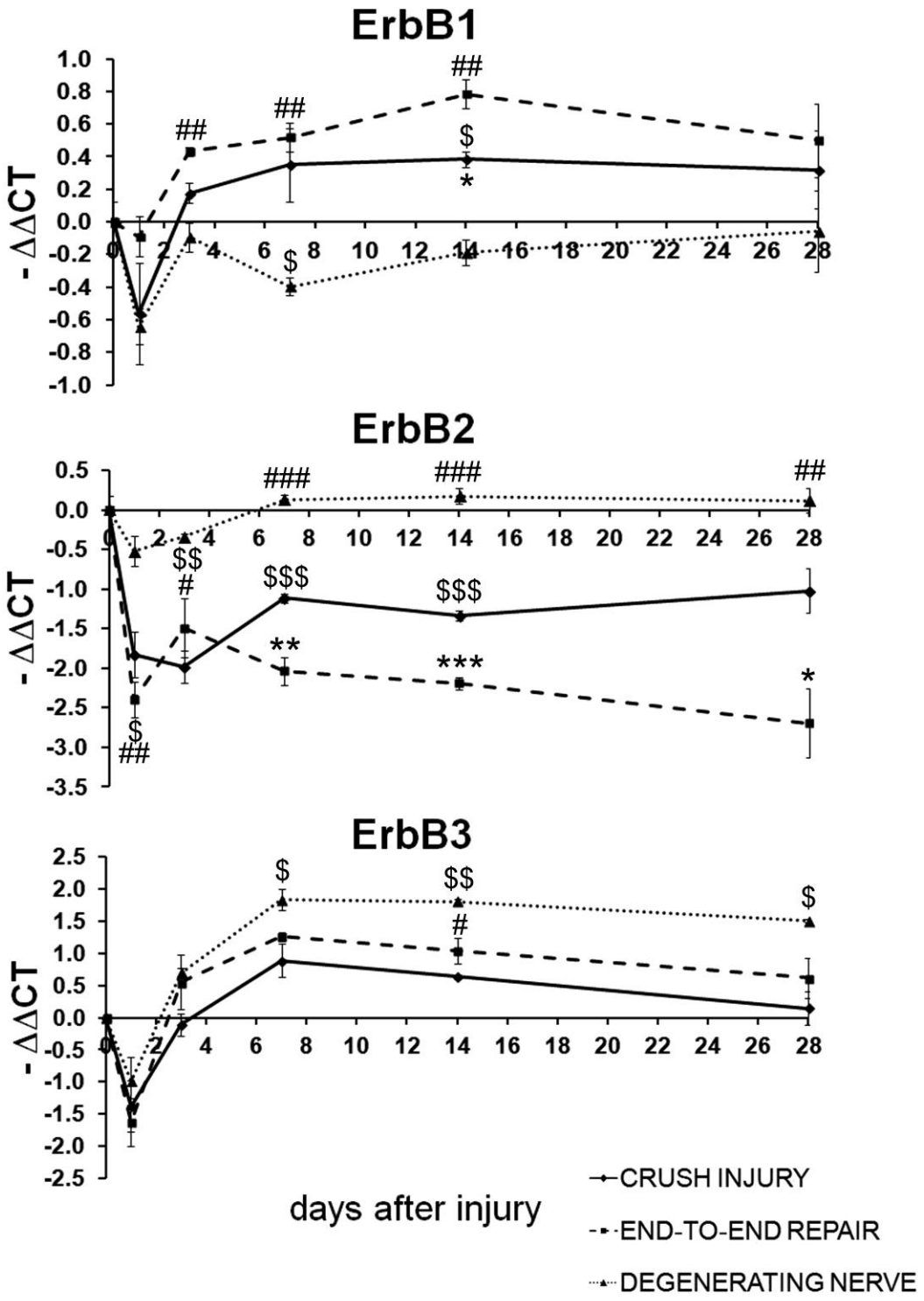
ErbB1
ErbB2
ErbB3
- ΔΔCT
days after injury
CRUSH INJURY
END-TO-END REPAIR
DEGENERATING NERVE

Figure 2

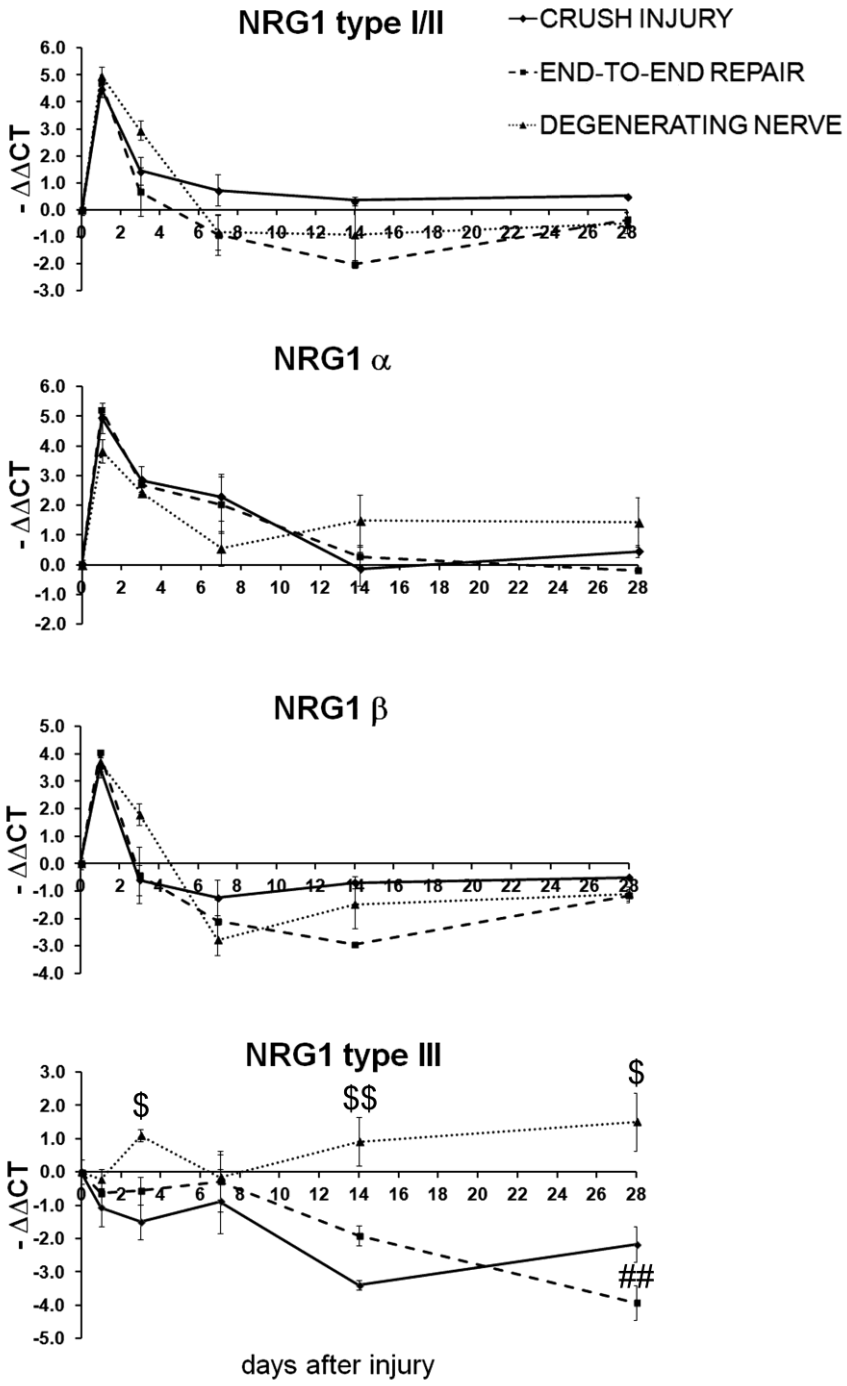
NRG1 type I/II
CRUSH INJURY
END-TO-END REPAIR
DEGENERATING NERVE
- ΔΔCT
NRG1 α
NRG1 β
NRG1 type III
$
$$
$
##
days after injury

Figure 3

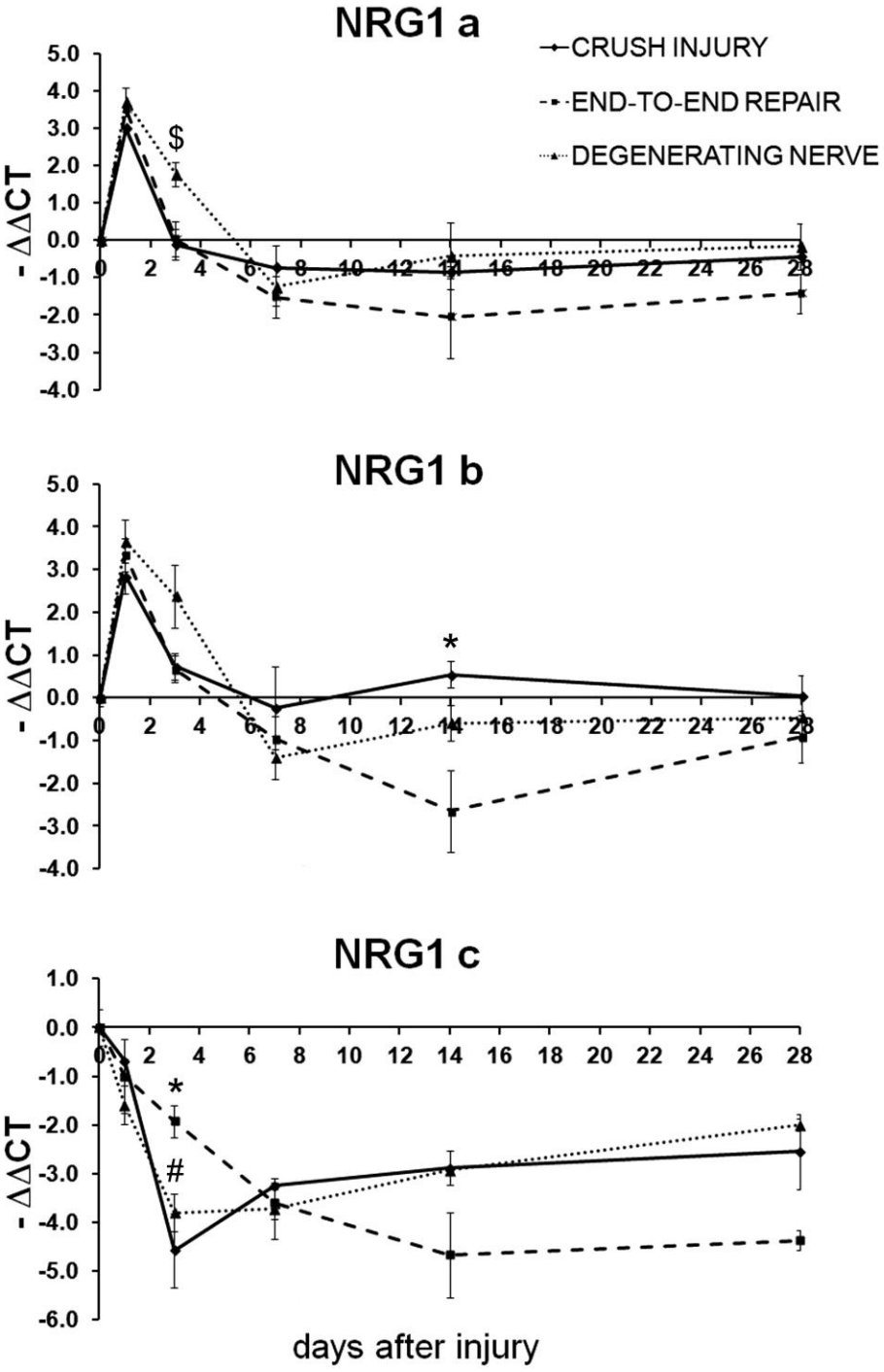
NRG1 a
CRUSH INJURY
END-TO-END REPAIR
DEGENERATING NERVE
- ΔΔCT
$
NRG1 b
*
NRG1 c
*
#
days after injury

Figure 4

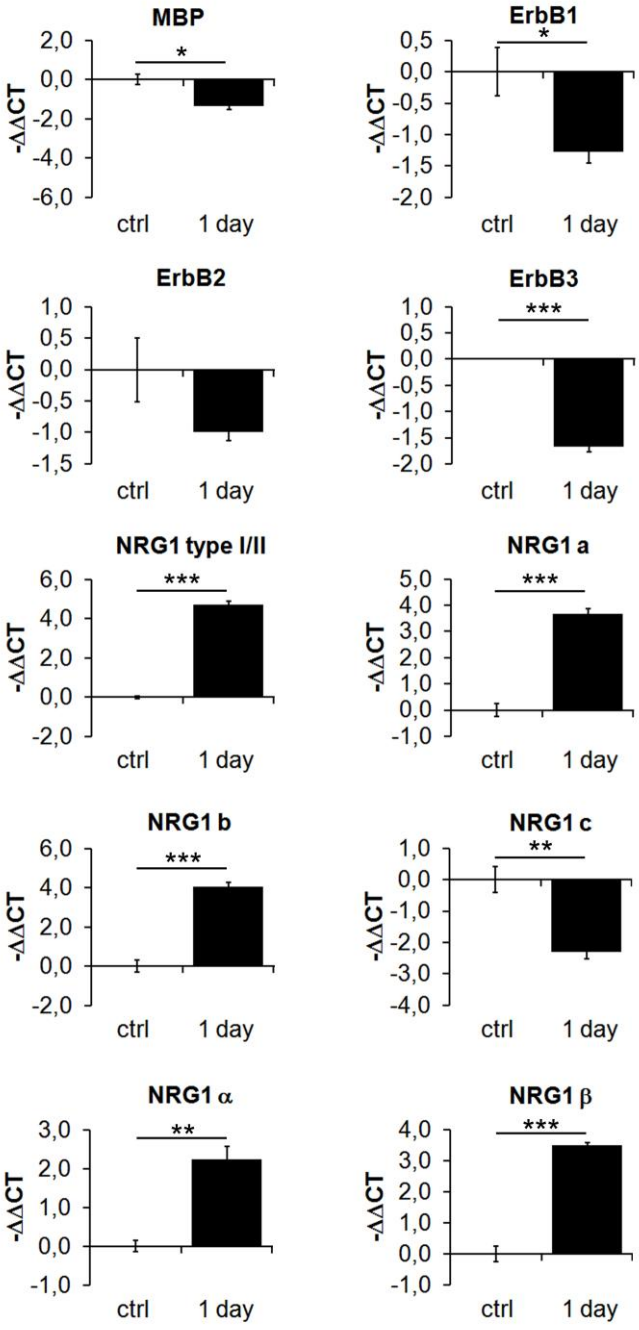
MBP
ErbB1
ErbB2
ErbB3
NRG1 type I/II
NRG1 a
NRG1 b
NRG1 c
NRG1 α
NRG1 β
-ΔΔCT
ctrl
1 day
*
**
***

Figure 5

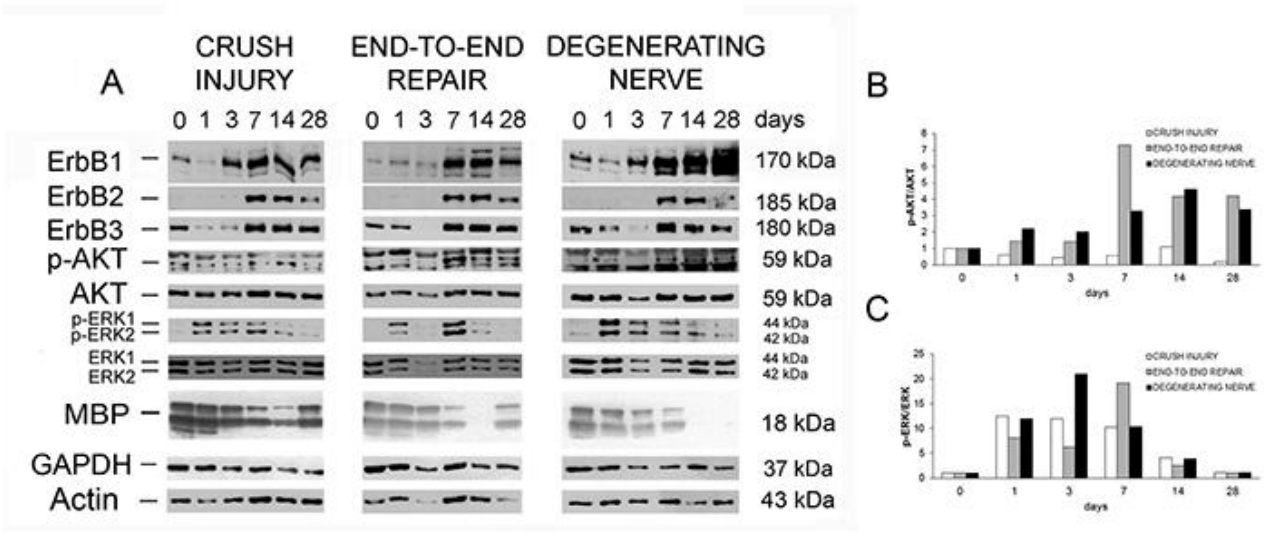
A
CRUSH INJURY
END-TO-END REPAIR
DEGENERATING NERVE
0 1 3 7 14 28
0 1 3 7 14 28
0 1 3 7 14 28
days
ErbB1
ErbB2
ErbB3
p-AKT
AKT
p-ERK1
p-ERK2
ERK1
ERK2
MBP
GAPDH
Actin
170 kDa
185 kDa
180 kDa
59 kDa
59 kDa
44 kDa
42 kDa
44 kDa
42 kDa
18 kDa
37 kDa
43 kDa
B
p-AKT/AKT
CRUSH INJURY
END-TO-END REPAIR
DEGENERATING NERVE
days
C
p-ERK/ERK
CRUSH INJURY
END-TO-END REPAIR
DEGENERATING NERVE
days

Figure 6

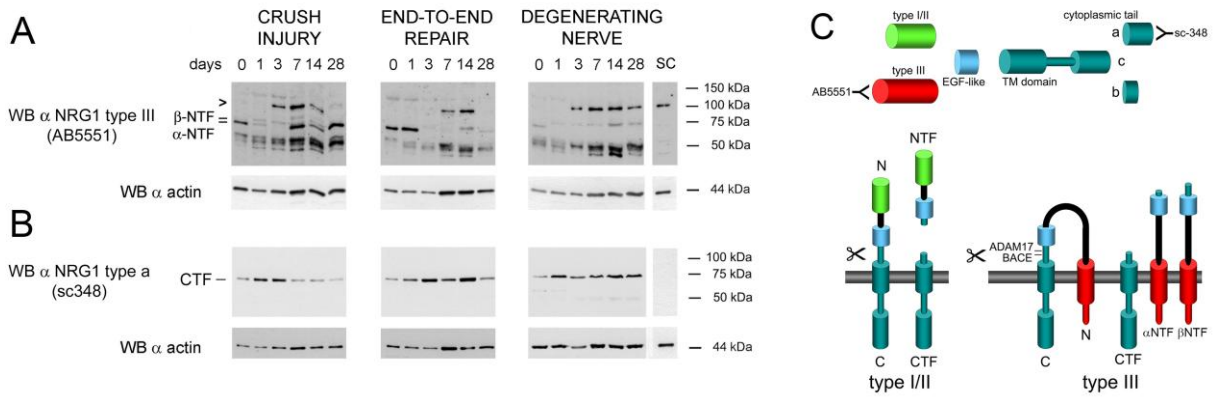
A
CRUSH INJURY
END-TO-END REPAIR
DEGENERATING NERVE
days 0 1 3 7 14 28
0 1 3 7 14 28
0 1 3 7 14 28 SC
WB α NRG1 type III (AB5551)
β-NTF >
α-NTF =
150 kDa
100 kDa
75 kDa
50 kDa
WB α actin
44 kDa
B
WB α NRG1 type a (sc348)
CTF –
100 kDa
75 kDa
50 kDa
WB α actin
44 kDa
C
type I/II
cytoplasmic tail
a
sc-348
type III
AB5551
EGF-like
TM domain
c
b
NTF
N
ADAM17
BACE
C
CTF
type I/II
N
αNTF βNTF
C
CTF
type III

Figure 7

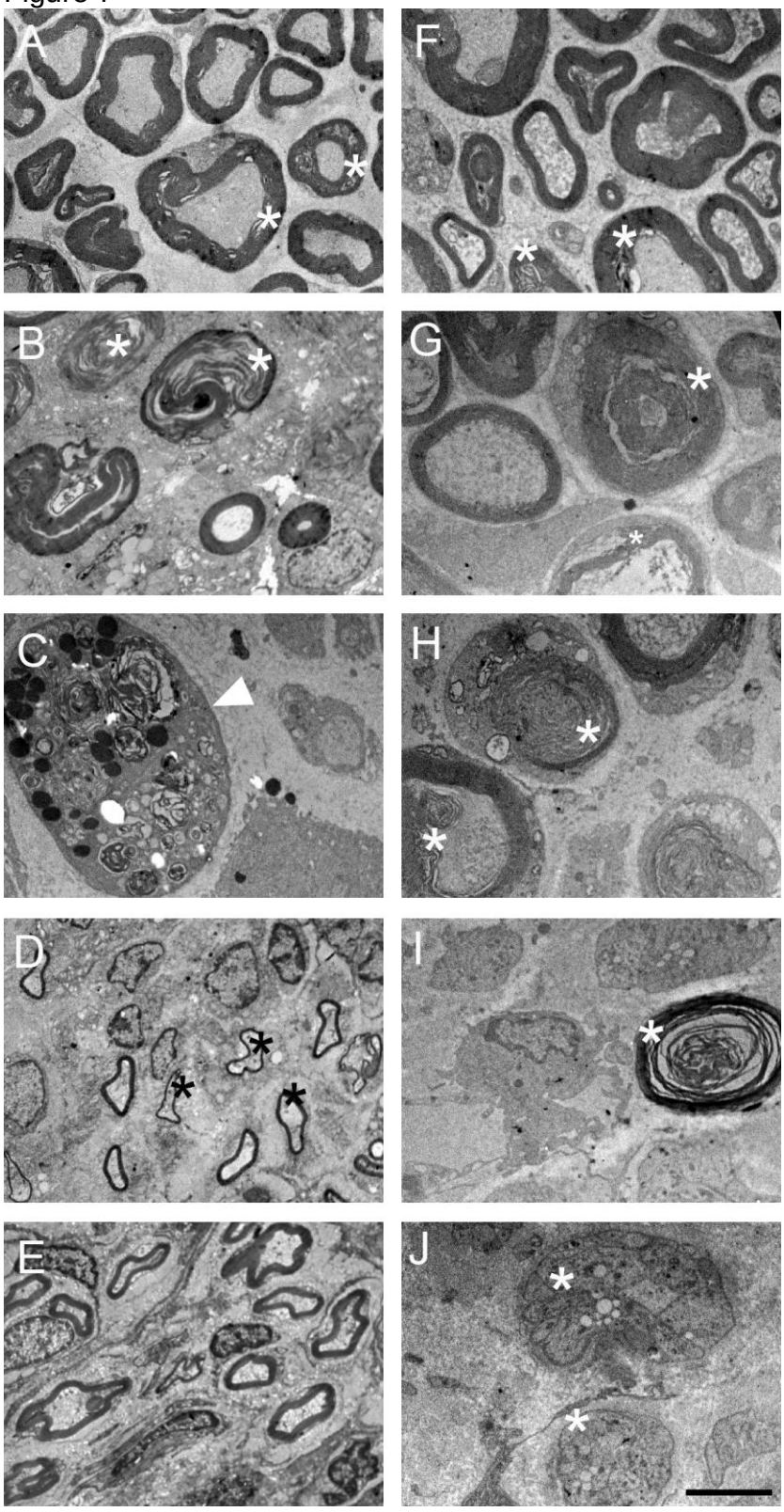

Figure 8

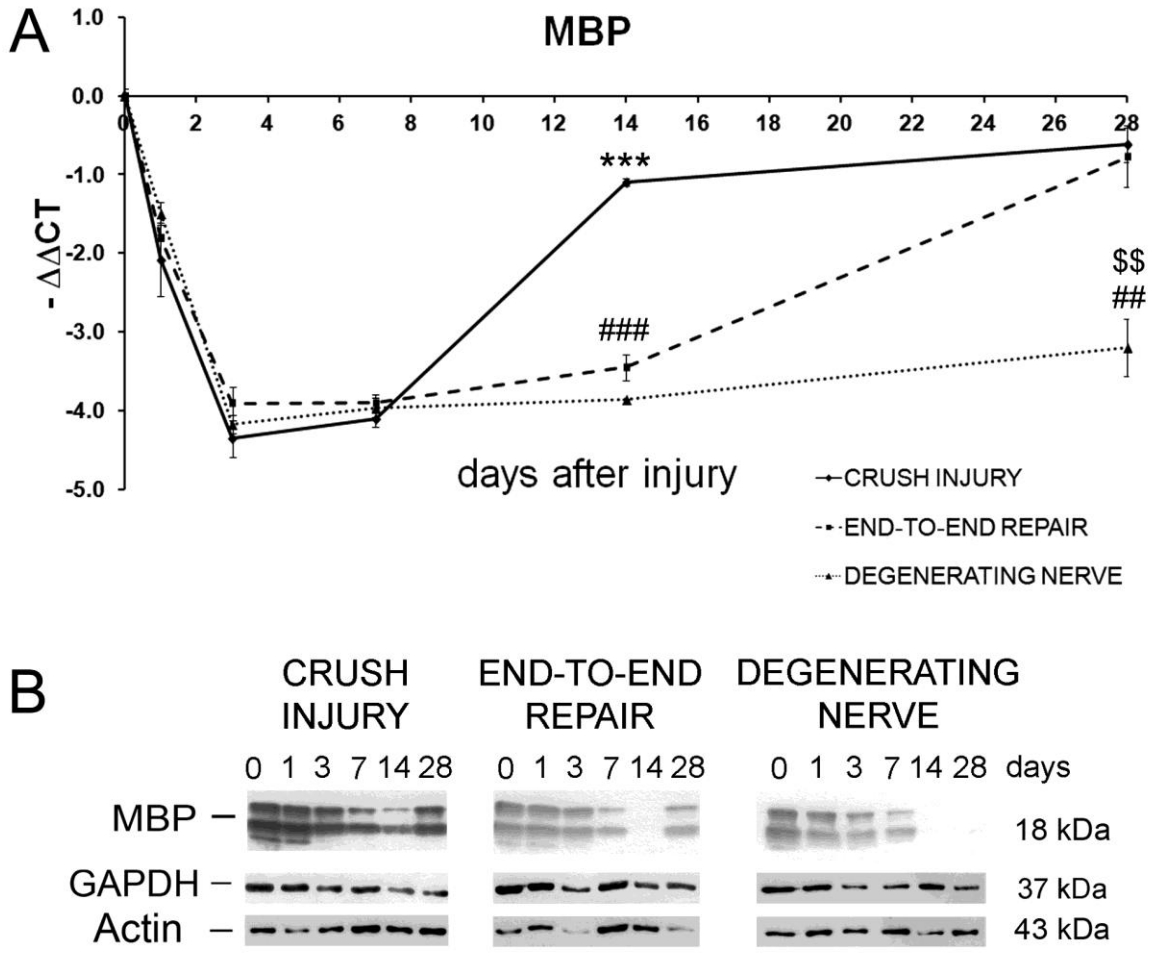
A
MBP
1.0
0.0
-1.0
-2.0
-3.0
-4.0
-5.0
- ΔΔCT
0 2 4 6 8 10 12 14 16 18 20 22 24 26 28
***
###
$$
##
days after injury
CRUSH INJURY
END-TO-END REPAIR
DEGENERATING NERVE
B
CRUSH INJURY
END-TO-END REPAIR
DEGENERATING NERVE
0 1 3 7 14 28
0 1 3 7 14 28
0 1 3 7 14 28 days
MBP
GAPDH
Actin
18 kDa
37 kDa
43 kDa

Figure 9

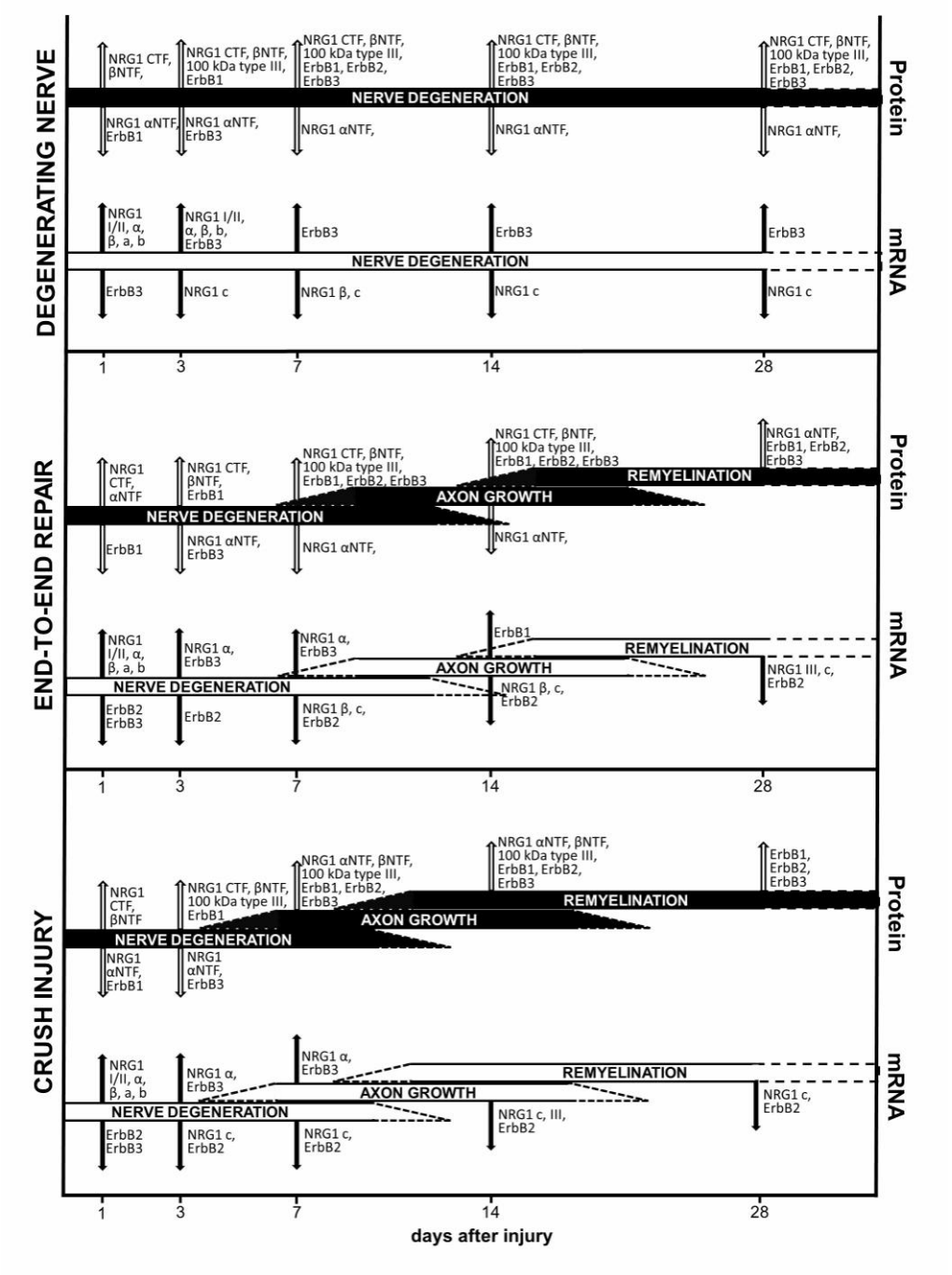
DEGENERATING NERVE
Protein
NRG1 CTF, βNTF,
NRG1 CTF, βNTF, 100 kDa type III, ErbB1
NRG1 CTF, βNTF, 100 kDa type III, ErbB1, ErbB2, ErbB3
NRG1 CTF, βNTF, 100 kDa type III, ErbB1, ErbB2, ErbB3
NRG1 CTF, βNTF, 100 kDa type III, ErbB1, ErbB2, ErbB3
NERVE DEGENERATION
NRG1 αNTF, ErbB1
NRG1 αNTF, ErbB3
NRG1 αNTF,
NRG1 αNTF,
NRG1 αNTF,
mRNA
NRG1 I/II, α, β, a, b
NRG1 I/II, α, β, b, ErbB3
ErbB3
ErbB3
ErbB3
NERVE DEGENERATION
ErbB3
NRG1 c
NRG1 β, c
NRG1 c
NRG1 c
1
3
7
14
28
END-TO-END REPAIR
Protein
NRG1 CTF, αNTF
NRG1 CTF, βNTF, ErbB1
NRG1 CTF, βNTF, 100 kDa type III, ErbB1, ErbB2, ErbB3
NRG1 CTF, βNTF, 100 kDa type III, ErbB1, ErbB2, ErbB3
NRG1 αNTF, ErbB1, ErbB2, ErbB3
REMYELINATION
AXON GROWTH
NERVE DEGENERATION
ErbB1
NRG1 αNTF, ErbB3
NRG1 αNTF,
NRG1 αNTF,
mRNA
NRG1 I/II, α, β, a, b
NRG1 α, ErbB3
NRG1 α, ErbB3
ErbB1
REMYELINATION
AXON GROWTH
NERVE DEGENERATION
NRG1 III, c, ErbB2
NRG1 β, c, ErbB2
ErbB2 ErbB3
ErbB2
NRG1 β, c, ErbB2
1
3
7
14
28
CRUSH INJURY
Protein
NRG1 CTF, βNTF
NRG1 CTF, βNTF, 100 kDa type III, ErbB1
NRG1 αNTF, βNTF, 100 kDa type III, ErbB1, ErbB2, ErbB3
NRG1 αNTF, βNTF, 100 kDa type III, ErbB1, ErbB2, ErbB3
ErbB1, ErbB2, ErbB3
REMYELINATION
AXON GROWTH
NERVE DEGENERATION
NRG1 αNTF, ErbB1
NRG1 αNTF, ErbB3
mRNA
NRG1 I/II, α, β, a, b
NRG1 α, ErbB3
NRG1 α, ErbB3
REMYELINATION
AXON GROWTH
NERVE DEGENERATION
NRG1 c, ErbB2
ErbB2 ErbB3
NRG1 c, ErbB2
NRG1 c, ErbB2
NRG1 c, III, ErbB2
1
3
7
14
28
days after injury

Table I

	Accession number	primer name	sequence 5'-3'	Amplicon size	Amplification efficiency
NRG1 type I/II	AF194993	rNRG1 I/II FW rNRG1 I/II/III REV	GGCGCAAACACTTCTTCATCCAC AAGTTTTCTCCTTCTCCGCGCAC	82	103%
NRG1 type III	AF194439	mrNRG1 III FW rNRG1 I/II/III REV	CCCTGAGGTGAGAACACCCAAGTC AAGTTTTCTCCTTCTCCGCGCAC	140	92%
NRG1 type alpha	AF194439	rNRG1-alfa/beta FW mrNRG1-alfa REV	TGCGGAGAAGGAGAAAACTTTC TTGCTCCAGTGAATCCAGGTTG	113	109%
NRG1 type beta	U02322 AY973245	rNRG1-alfa/beta FW mrNRG1-beta REV	TGCGGAGAAGGAGAAAACTTTC AACGATCACCAGTAAACTCATTTGG	119	103%
NRG1 type a	U02322	mrNRG1 exon C3 FW rNRG1 exon a REV	CCCCTGACTCCTACAGAGACTCTCC TAGGGGAGCTTGGCGTGTGG	107	100%
NRG1 type b	AY973245	mrNRG1 exon C3 FW rNRG1 exon b REV	CCCCTGACTCCTACAGAGACTCTCC AGGGTCTAAGATGAGTTGCTGACAGC	126	101%
NRG1 type c	U02324	mrNRG1 exon C3 FW rNRG1 exon c REV	CCCCTGACTCCTACAGAGACTCTCC CCGCAGGTGCTCATGGGATTC	108	104%
ErbB1	NM_031507	rErbB1 FW rErbB1 REV	CACCACGTACCAGATGGATG CGTAGTTTCTGGGGCATTTC	83	103%
ErbB2	NM_017003	rErbB2 FW rErbB2 REV	TGACAAGCGCTGTCTGCCG CTTGTAGTGGGCGCAGGCTG	106	100%
ErbB3	NM_017218	mrErbB3 FW mrErbB3 REV	CGAGATGGGCAACTCTCAGGC AGGTTACCCATGACCACCTCACAC	129	93%
MBP	NM_001025291	mrMBP FW rMBP REV	GGACCCAAGATGAAAACCCAGTAGTCC CCTTTCCTTGGGATGGAGGGGG	81	98%
ANKRD27	NM_001271264	rAnkrd27 FW rAnkrd27 REV	CCAGGATCCGAGAGGTGCTGTC CAGAGCCATATGGACTTCAGGGGG	95	99%
RICTOR	XM_001055633	rRICTOR FW rRICTOR REV	GAGGTGGAGAGGACACAAGCCC GGCCACAGAACTCGGAAACAAGG	81	106%